Antibacterial tooth surface created by laser-assisted pseudo-biomineralization in a supersaturated solution

Ayako Oyane[1,*], Ikuko Sakamaki[1], Kenji Koga[1], Maki Nakamura[1],

Kanako Shitomi[2], Hirofumi Miyaji[2]

[1]*Nanomaterials Research Institute, National Institute of Advanced Industrial Science and Technology (AIST), Central 5, 1-1-1 Higashi, Tsukuba, Ibaraki 305-8565, Japan*

[2]*Department of Periodontology and Endodontology, Faculty of Dental Medicine, Hokkaido University, N13W7, Kita-ku, Sapporo, Hokkaido 060-8586, Japan*

* Corresponding author: **Ayako Oyane, Ph.D.,**

Nanomaterials Research Institute, National Institute of Advanced Industrial Science and Technology (AIST), Central 5, 1-1-1 Higashi, Tsukuba, Ibaraki 305-8565, Japan

Tel:+81-29-861-3005, Fax:+81-29-861-3005, E-mail: a-oyane@aist.go.jp

ABSTRACT

A technique for implementing biocompatible and antibacterial functions to a targeted region on tooth surfaces has potential in dental treatments. We have recently demonstrated pseudo-biomineralization, *i.e.*, the growth of an apatite layer on a human dentin substrate by a laser-assisted biomimetic (LAB) process, based on pulsed laser irradiation in a supersaturated CaP solution. In this study, pseudo-biomineralization was induced in the presence of fluoride ions using the LAB process in order to fabricate an antibacterial fluoride-incorporated apatite (FAp) layer on the dentin surface. After processing for 30 min, a micron-thick FAp layer was formed heterogeneously at the laser-irradiated solid−liquid interface *via* pseudo-biomineralization. A time-course study revealed that the LAB process first eliminated the pre-existing organic layer, while allowing fluoride incorporation into the dentin surface within 1 min. Within 5 min, FAp nanocrystals precipitated on the dentin surface. Within 30 min, these nanocrystals acquired a pillar-like structure that was weakly oriented in the direction normal to the substrate surface to form a dense micron-thick layer. This layer was integrated seamlessly with the underlying dentin without any apparent gaps. The FAp layer exhibited antibacterial activity against a major oral bacterium, *Streptococcus mutans*. The proposed LAB process is expected to be a useful new tool for tooth surface functionalization *via* facile and area-specific pseudo-biomineralization.

Keywords: hydroxyapatite, fluoride, calcium phosphate (CaP), dentin, laser, biomimetic process, coating

Abbreviations

FAp, Fluoride-incorporated apatite; LAB, Laser-assisted biomimetic; CaP, Calcium phosphate; CP solution, Supersaturated calcium phosphate solution; *S. mutans*, *Streptococcus mutan*; AIST, Advanced Industrial Science and Technology; EDTA, Ethylenediaminetetraacetic acid; FCP solution, Supersaturated calcium phosphate solution supplemented with NaF; ICP-OES, inductively coupled plasma-optical emission spectroscopy; SEM, Scanning electron microscope; EDX, Energy-dispersive X-ray; XRD, X-ray diffraction; FT-IR, Fourier transform infrared spectroscopy; ATR, Attenuated total reflection; FIB, Focused ion beam; TEM, Transmission electron microscopy; HAADF, High-angle annular dark field; STEM, Scanning transmission electron microscopy; BHI, Brain heart infusion; CFU, Colony-forming unit; OCP, Octacalcium phosphate;

1. Introduction

Periodontal disease is a chronic infection and occurs in the majority of elderly people worldwide [1]. In its early stage, a bacterial biofilm and/or dental plaque are formed on the tooth, causing inflammation in the gum. As inflammation progresses into the supporting connective and alveolar bone tissues, a periodontal pocket (cavity at the gum–tooth interface) is formed and becomes enlarged as a consequence of loss of the periodontal attachment. In severe cases, the supporting alveolar bone deteriorates, resulting in tooth loosening and eventually tooth loss if left untreated. In surgical periodontal treatments, a periodontal pocket is cleaned by removal of the biofilm, dental plaque, and calculus from the infected tooth (root) surface either manually, chemically, or mechanically. However, a surface-treated tooth root has poorer biocompatibility than a healthy natural tooth, and thus, the periodontal attachment is rarely reconstructed [2−4]. The persisting periodontal pocket remains a major risk factor for recurrence of periodontal disease.

We believe that fluoride-incorporated apatite (FAp) coating on a surface-treated tooth root would be effective in reducing the risk of periodontal disease recurrence for the following reasons. Apatite is a calcium phosphate compound found in human dentin, enamel, and cementum. Apatite [more specifically, sintered hydroxyapatite: $Ca_{10}(PO_4)_6(OH)_2$] has long been used as a biomaterial for orthopedic and dental applications owing to its excellent biocompatibility with both soft and hard living tissues [5−8]. For instance, apatite coating has been applied to commercial dental implants to accelerate osseointegration [5,6]. Fluoride ions are known to substitute for hydroxyl ions in apatite, thereby improving its chemical durability (acid-resistance) and hardness [9,10]. In addition, fluoride ions exhibit antibacterial properties against various types of bacteria including periodontopathic bacteria [11], and are widely used for oral and dental healthcare [12]. It is

therefore highly anticipated that a FAp coating on a tooth root surface would enhance the reconstruction of a periodontal attachment, while repelling bacteria from the periodontal tissues.

Various techniques have been proposed to create an artificially mineralized tooth surface [13-25]. These techniques include physical coating techniques such as pulsed laser deposition [13], powder jet deposition [14], and apatite sheet adhesion [15], and chemical techniques based on pseudo-biomineralization [16-23]. In general, physical techniques are weak in the coating adhesion and integration with a tooth surface, whereas chemical techniques are time-consuming. Pseudo-biomineralization techniques in combination with laser processing have also been proposed as physicochemical techniques [24,25]. However, it is still difficult to find a technique that meets all the requirements for chair-side FAp coating for tooth surface functionalization, *i.e.*, simplicity (single step), rapidness (in half an hour), use of orally administrable sources, area-specific coating capability, and fine integration between the resulting coating and a tooth surface.

Recently, we developed a laser-assisted biomimetic (LAB) process [26] that is likely to be suitable for chair-side FAp coating on a tooth surface. In the LAB process, a substrate surface is irradiated for a few tens of minutes with low-energy Nd:YAG pulsed laser light in a supersaturated calcium phosphate (CaP) solution (referred to as CP solution [26,27]). This process has enabled facile ($\leq$ 30 min) and area-specific CaP coating on various artificial materials under standard ambient pressure and temperature [26,28-35]. More recently, we applied this LAB process to a substrate of human dentin and demonstrated rapid pseudo-biomineralization, *i.e.*, apatite formation, on the surface [36]. However, in that preliminary study, the processing time was fixed at 30 min; therefore, the time course and mechanism of laser-assisted pseudo-biomineralization remain to be elucidated.

In this study, the LAB process was performed using CP solution supplemented with NaF to achieve facile FAp coating on a dentin substrate *via* pseudo-biomineralization in the presence of fluoride ions. To elucidate the time course and mechanism of pseudo-biomineralization, the processing time was varied from 1 to 30 min and surface and cross-sectional analyses were conducted on the LAB-processed dentin substrates. The area-specific coating capability and antibacterial activity of the processed substrates were also assayed to demonstrate the potential of the LAB process in tooth surface functionalization. In this preliminary antibacterial assay, *Streptococcus mutans* (*S. mutans*) was used as a model bacterium because it is one of major oral bacteria involving the bacterial coaggregation and initial biofilm formation [37,38].

2. Materials and methods

2.1. Preparation of dentin substrates

As human dentin sources, donated third molars extracted in standard treatments from patients older than 40 years at the dental department of Hokkaido University Hospital were used after obtaining informed consent. All the experiments were conducted under conditions approved by the ethical review boards of both the Hokkaido University Hospital for clinical research (approval No. 16-72) and the National Institute of Advanced Industrial Science and Technology (AIST).

Tabular substrates (*ca.* 1 mm in thickness) of human dentin were prepared by cutting the third molar with a diamond disk (Horico diamond disk 87xFSI, HORICO DENTAL Hopf, Ringleb & Co. GmbH & Cie., Germany). The dimensions of the substrates were either 3–5 × 5 mm (size S), 5 × 5 mm (size M), or 6–8 × 10–11 mm (size L). The S-sized substrates were used in the following experiments unless otherwise indicated. The substrates were polished with #600 and #2000 SiC polishing papers (FUJI STAR DCCS, Sankyo-Rikagaku Co., Ltd, Japan), and washed

ultrasonically with pure water using an ultrasonic cleaner (VS-100III, AS ONE Corporation, Japan). They were then treated ultrasonically for 5 min with a 3% ethylenediaminetetraacetic acid (EDTA) solution (Smear Clean, Nippon Shika Yakuhin Co., Ltd., Japan) for smear removal followed by final ultrasonic cleaning with pure water. The EDTA solution is a clinically approved smear removal agent that is used in various dental treatments including periodontal treatments. The thus-prepared dentin substrates were kept at −20°C before use.

2.2. Preparation of CP solution supplemented with NaF (FCP solution)

A fluoride-free CP solution was first prepared as a mother solution using reagent-grade chemicals (all purchased from NACALAI TESQUE, Inc., Japan) according to previous reports [27,36]. The CP solution was prepared by dissolving NaCl (final concentration = 142 mM), $K_2HPO_4 \cdot 3H_2O$ (1.50 mM), 1 M HCl (40 mM), and $CaCl_2$ (3.75 mM) in ultrapure water and buffering the solution to pH = 7.40 at 25 °C with tris(hydroxymethyl)aminomethane (final concentration = 50 mM) and a necessary amount of 1 M HCl. The as-prepared CP solution was stored in a sealed polystyrene container at 4 °C before use for a maximum of 1 month.

Before each LAB process, the CP solution was supplemented with NaF (final concentration = 1.0 mM). The slight increase in solution volume was ignored when calculating the final NaF concentration. The solution was stirred for a few minutes, and then filtered through a 0.22-μm pore-size filter. The solution (referred to as FCP solution; same solution as “F1000” in Reference 21) was used immediately for the LAB process.

2.3. LAB process for FAp coating

The LAB process was performed as described in our previous reports [34,36]. Each substrate was placed on the bottom of a glass bottle using a poly(tetrafluoroethylene) sample holder. The FCP solution (5 mL) was poured into the bottle to fully immerse the substrate in the solution. The bottle was set in a temperature-controlled water bath (25 °C), and the substrate surface was irradiated with nanosecond pulsed laser light (λ = 355 nm, 30 Hz) with a fluence of 0.2 J/cm^2 per pulse (6 W/cm^2) using a Nd:YAG laser (Quanta-Ray LAB-150-30, Spectra-Physics, USA). These irradiation conditions were determined according to our preliminary optimization studies using a sintered hydroxyapatite substrate [29,34]. The laser beam had an output diameter of approximately 8 mm. For the S- and M-sized substrates, the laser beam was used without focusing or masking in order to entirely irradiate one surface. For the L-sized substrates, the laser beam was passed through a 5-mm diameter hole in a metallic mask without focusing in order to irradiate only a small circular region of the surface. The irradiation time was varied from 1 to 30 min, after which the substrate was removed from the solution, washed gently with ultrapure water, and air-dried at room temperature.

2.4. Chemical analyses of the FCP solution

The FCP solution was analyzed for residual Ca and P after 30 min of the LAB process. Immediately after the LAB process, an adequate amount (estimated from the change in total mass) of ultrapure water was added to the residual FCP solution to compensate for water loss due to evaporation. The solution was analyzed for Ca and P concentrations using inductively coupled plasma-optical emission spectroscopy (ICP-OES; ULTIMA2, HORIBA, Ltd., Japan). The pristine FCP solution was also analyzed as a control. The residual ratio (%) of Ca and P in the FCP solution after the LAB process was calculated from the difference in the Ca and P concentrations between

the pristine and residual FCP solutions. The results were expressed as the mean of two independent experiments using the M-sized substrates.

2.5. Surface analyses of the substrates

The surfaces of the substrates before and after the LAB process were analyzed using scanning electron microscopy (SEM; S-4800, Hitachi High-Technologies Corporation, Japan) in conjunction with energy-dispersive X-ray (EDX) analysis (EMAX x-act, HORIBA, Ltd., Japan), X-ray diffraction (XRD; M18X, MacScience, Japan) with CuKα radiation, and Fourier transform infrared spectroscopy (FT-IR; FT/IR-4700, JASCO Corporation, Japan). The FT-IR spectrophotometer was equipped with an attenuated total reflection (ATR) accessory with a monolithic diamond crystal. Prior to SEM-EDX analyses, the substrates were sputter-coated with carbon using a carbon coater (VC-100, Vacuum Device Co., Ltd., Japan).

2.6. Ultrastructural cross-sectional analyses

Cross-sectional ultra-thin samples were prepared from the LAB-processed substrates using a focused ion beam (FIB) technique with a Ga^+ ion source (FB-2100, Hitachi, Japan). As a pretreatment, the substrate was coated manually with a Cr-containing oil-based ink to protect the surface. The substrate was then coated with tungsten using $W(CO)_6$ gas. A cross-sectional sample was prepared from the substrate, fixed on a molybdenum FIB lift-out grid, and thinned to approximately 100 nm.

The cross-sectional ultra-thin samples were analyzed using an analytical transmission electron microscopy (TEM; Tecnai Osiris, FEI, USA) system operating at 200 kV and equipped with an EDX spectrometer (Super-X system, FEI, USA) and a high-angle annular dark field (HAADF)

scanning transmission electron microscopy (STEM) system with a probe diameter of less than 1 nm. For comparison, we used cross-sectional STEM-EDX data for an unprocessed (as-prepared) dentin substrate obtained in our previous study [36]. In the quantitative analysis by STEM-EDX, three different regions in each sample were analyzed to obtain the mean and the standard deviation (SD).

2.7. Antibacterial assay

The antibacterial properties of the LAB-processed (30 min) substrate were assayed using a facultative anaerobic bacterium, *S. mutans* (ATCC® 35668™, ATCC, USA). The unprocessed substrate (as-prepared substrate) was used as a control. For each group, four substrates (M-size) were tested. As a culture medium, a brain heart infusion (BHI) broth (PEARLCORE, Eiken Chemical, Co., Ltd., Japan) supplemented with 1% sucrose and 0.1% antibiotic (gramicidin D and bacitracin, FUJIFILM Wako Pure Chemical Corporation Ltd., Japan) was used.

An antibacterial assay was performed using a conventional colony-forming unit (CFU) method. The substrates were sterilized by UV light irradiation before the assay. Each substrate was placed in the well of a 48-well plate, and 0.5 mL of the bacterial suspension (4.0×10^6 CFU/mL) was added to each well. After anaerobic culture at 37 °C for 12 h, the bacterial suspension containing the substrate was ultrasonicated for 10 s, diluted (from 1/10 to $1/10^7$) with the BHI broth, and inoculated on an agar culture medium. After anaerobic culture at 37 °C for 24 h, the number of bacterial colonies was counted to estimate the CFU. Data sets obtained by $1/10^7$ dilution were compared using Student's t-test, and the decrease in CFU with respect to the control was considered statistically significant when the p-value was less than 0.05.

3. Results and Discussion

3.1. Surface analyses

The LAB process modified the dentin surface at the microscopic level within only 5 min. SEM observations revealed micron-sized dentinal canaliculi (also called dentinal tubules) on the dentin surface (see arrows in Figure 1a). The flat region of the dentin surface was fairly smooth before the LAB process and remained unchanged after processing for 1 min. After processing for 5 min, the dentin surface was roughened at the submicron scale. The surface roughness increased with processing time to 30 min; the dentin surface was filled with densely assembled submicron particles with diameters of a few hundred nanometers. SEM-EDX spectra from the dentin surface showed strong peaks due to O, P, and Ca, all of which are component elements of apatite, irrespective of the processing time (Figure 1b). In addition to these peaks, a small peak due to F

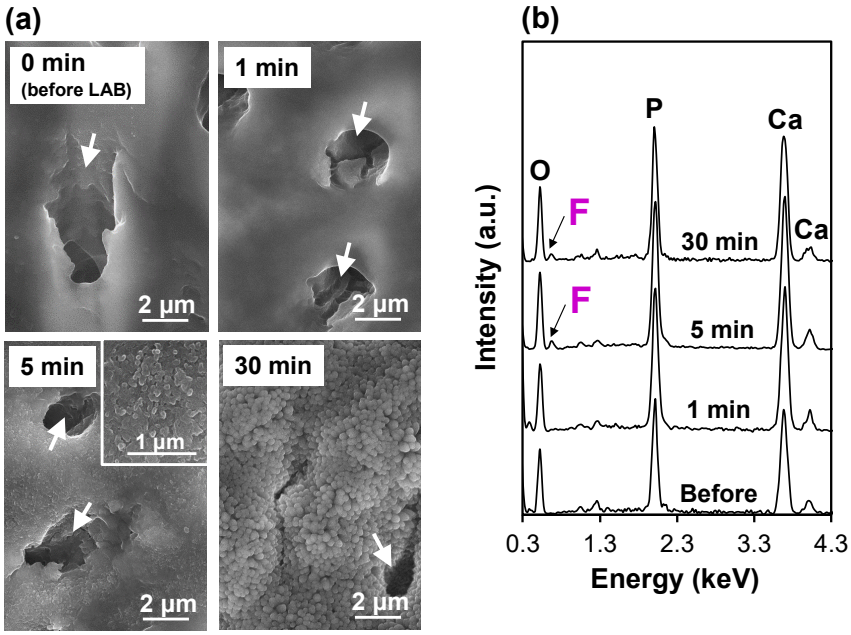

Figure 1. (a) SEM images and (b) SEM-EDX spectra of the dentin substrate surfaces before and after the LAB process for various times up to 30 min. The inset in (a) shows a magnified image and the arrows indicate dentinal tubules.

appeared for the substrate processed for 5 min, suggesting fluoride incorporation onto the dentin surface.

The submicron particles observed on the LAB-processed (30 min) dentin substrate were CaP-based precipitates formed heterogeneously on the dentin surface by consuming Ca and P in the metastable FCP solution. This was confirmed by ICP-OES, which indicated that both Ca and P concentrations in the FCP solution decreased by approximately 10% after the LAB process for 30 min (Figure 2a). During the LAB process for 30 min, the FCP solution remained transparent without inducing homogeneous CaP precipitation. Thus, the CaP precipitation occurred heterogeneously at the dentin surface, *i.e.*, at the laser-irradiated solid−liquid interface, which is described in Section 3.3.

The CaP-based submicron particles on the LAB-processed (30 min) dentin substrate were composed of FAp crystals. The dentin substrates were analyzed using FT-IR and XRD before and after the LAB process for 30 min. In the FT-IR spectra (Figure 2b), the unprocessed substrate showed peaks ascribed to amide and phosphate groups from dentinal collagen and apatite, respectively. The former peak from collagen decreased, whereas the latter peak from apatite increased after the LAB process. All the peaks in the XRD patterns were indexed to apatite (Figure 2c). Other CaP phases such as octacalcium phosphate (OCP; main peak position at 4.7°) were not detected in either the unprocessed substrate or the LAB-processed substrate (Figures 2c and 2d). The apatite peaks increased in both intensity and sharpness after the LAB process (Figure 2c). Among these, the apatite 002 diffraction peak at approximately 26° in particular increased after the LAB process. This is due to the *c*-axis orientation of the apatite crystals in the surface layer, as described in Section 3.2.3.

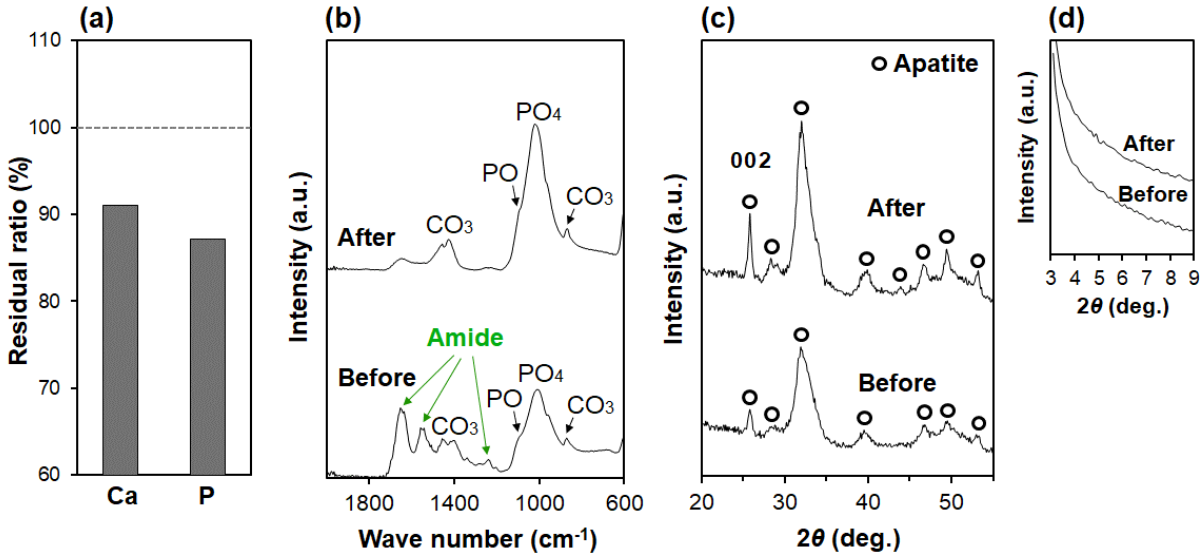

Figure 2. (a) Residual ratio (%) of Ca and P in the FCP solution after the LAB process for 30 min (determined by ICP-OES), (b) FT-IR spectra, and (c, d) $2\theta/\theta$ XRD patterns (c: larger angle region, d: smaller angle region) of the dentin substrate surfaces before and after the LAB process for 30 min.

3.2. Cross-sectional analyses

3.2.1 Initial stage of the LAB process (0–1 min)

The LAB process induced the formation of a F-rich surface layer on the dentin substrate while diminishing the preexisting N-rich organic layer within 1 min. As reported previously [36], the as-prepared substrate had a N-rich organic layer on its surface due to surface demineralization

(dissolution of dentinal apatite) during the prior cleaning with EDTA. The N-rich organic layer was approximately 300 nm thick, as visualized by the N distribution (yellow) in the cross-sectional STEM-EDX elemental map (Figure 3a). The inner region underneath the N-rich organic layer is the dentin according to the elemental distributions of Ca (red) and P (green). The uppermost Cr-rich layer (blue) is the Cr-containing oil-based ink that was put on the substrate to protect its surface in the preparation of the cross-sectional ultra-thin samples as described in Section 2.6. The STEM-EDX spectra (Figure 3c) show that the N-rich organic layer was deficient in apatite components (Ca and P) and was composed mainly of C and N, which was different from the inner dentin region. Trace amounts of heavy elements Ga, W, and Mo were detected as contaminants derived from FIB and the TEM grid. After the LAB process for 1 min, the N-rich organic layer

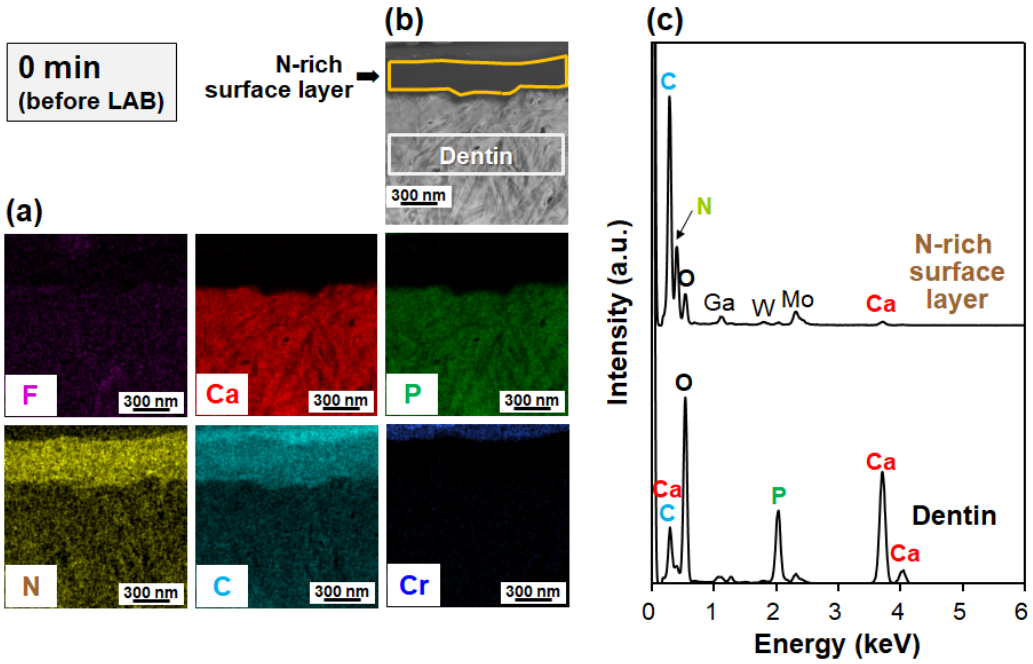

Figure 3. (a) Cross-sectional STEM-EDX elemental maps, (b) corresponding HAADF image, and (c) STEM-EDX spectra of the unprocessed dentin substrate (as-prepared substrate) surface. The EDX spectra in (c) were obtained respectively from the N-rich surface layer (brown-boxed region) and dentin (gray-boxed region) in (b).

(yellow) almost disappeared as it became thinner (<50 nm) and was observed dimly on the dentin surface (Figure 4a). At the same time, a F-rich layer (purple) appeared on the dentin surface. This F-rich surface layer was thicker (50−100 nm) than the N-rich organic layer and was partly overlapped with the N-rich region and the underlying Ca- and P-rich regions. The F-rich surface layer was quite similar in composition to the underlying dentin, except for the F content; F was clearly detected in the surface layer but not in the underlying dentin (Figure 4c). The F/P atomic ratio was 0.19 ± 0.02 in the F-rich surface layer and 0.02 ± 0.00 in the underlying dentin.

In this very initial stage of the LAB process within 1 min, the formation of CaP crystals on the dentin surface was not obvious in the TEM images. Figure 5 shows a time-course of the cross-sectional surface structure of the dentin substrate during the LAB process up to 30 min. The

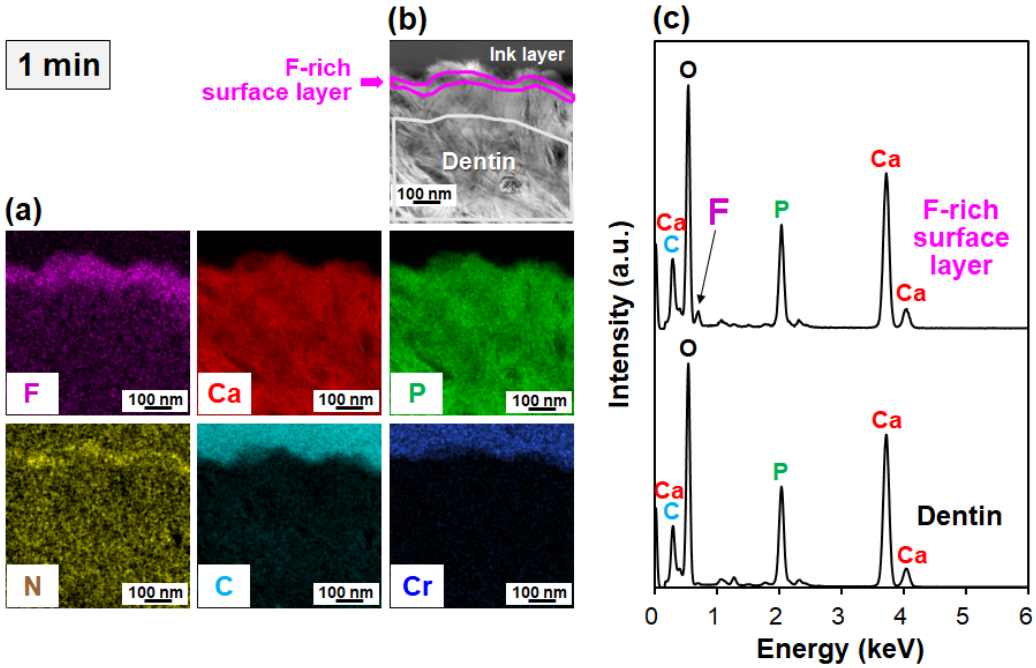

Figure 4. (a) Cross-sectional STEM-EDX elemental maps, (b) corresponding HAADF image, and (c) STEM-EDX spectra of the dentin substrate surface after the LAB process for 1 min. The EDX spectra in (c) were obtained respectively from the F-rich surface layer (purple-boxed region) and dentin (gray-boxed region) in (b).

unprocessed substrate (upper left image) showed bundles of fine needle-like crystals, which are typical of *c*-axis-oriented dentinal apatite nanocrystals. The LAB-processed (1 min) substrate had a similar structure (upper middle image) without any noticeable precipitates on its surface.

3.2.2 Second stage of the LAB process (5 min)

The F-rich surface layer thickened (>100 nm) after 5 min of the LAB process, whereas the preexisting N-rich organic layer became undetectable. As revealed by the Ca, P, and Cr distributions in Figure 6a, the top ink layer (blue) is located directly above the dentin substrate (red and green) without any interstitial spaces between them. The N-rich layer disappeared completely from the interface between the ink layer and the underlying dentin. In contrast, the F-rich layer (purple) became thicker (>100 nm) as the processing time increased from 1 to 5 min. This submicron F-rich layer overlapped with the Ca- and P-rich regions, which suggests the coexistence

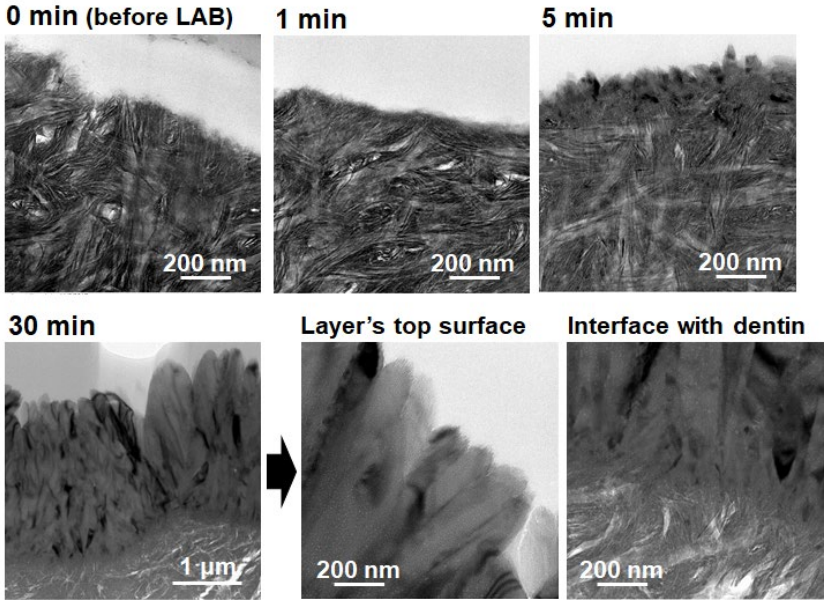

Figure 5. Cross-sectional TEM images of the dentin substrates before and after the LAB process for various times up to 30 min. The magnification of the lower left image was reduced to show the surface layer thickness.

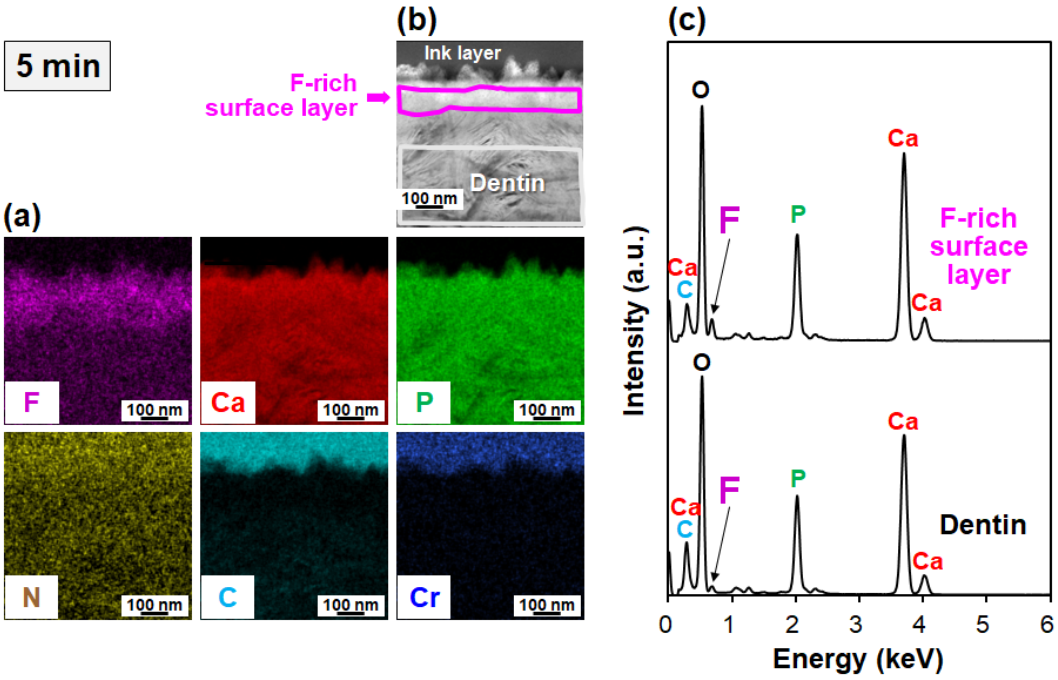

Figure 6. (a) Cross-sectional STEM-EDX elemental maps, (b) corresponding HAADF image, and (c) STEM-EDX spectra of the dentin substrate surface after the LAB process for 5 min. The EDX spectra in (c) were obtained respectively from the F-rich surface layer (purple-boxed region) and dentin (gray-boxed region) in (b).

of these elements. Figure 6c shows that the F-rich submicron layer was composed of CaP with a higher F content (F/P atomic ratio = 0.22 ± 0.02) than the underlying dentin (F/P atomic ratio = 0.08 ± 0.01).

The submicron F-rich layer formed on the LAB-processed (5 min) dentin surface was composed of FAp nanocrystals. As depicted in the upper right image in Figure 5, a number of nanosized precipitates, thicker than the needle-like nanocrystals of dentinal apatite, emerged on the dentin surface after processing for 5 min. The selected-area electron diffraction (SAED) pattern obtained from the precipitates (upper left circle in Figure 7a) was ascribed to crystalline apatite with larger grains (Figure 7b). Figure 7d shows a high-resolution TEM (HRTEM) image obtained

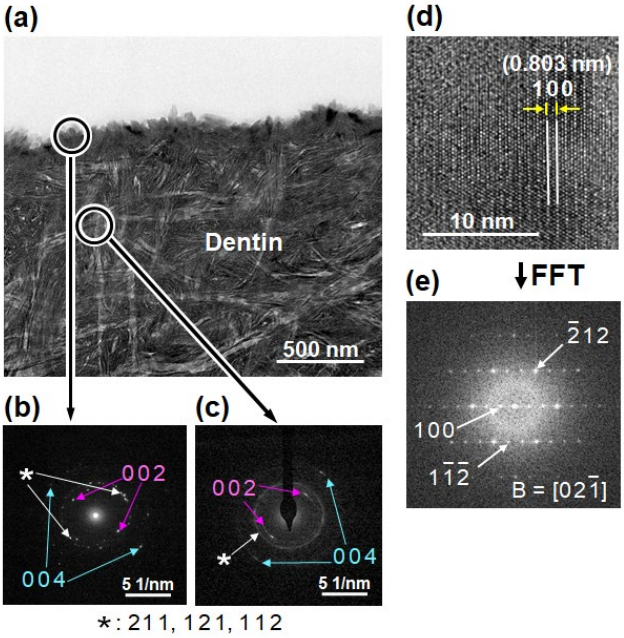

Figure 7. (a) Cross-sectional TEM image of the dentin substrate surface after the LAB process for 5 min, (b,c) SAED patterns obtained from the circled areas in (a), (d) HRTEM image obtained from the surface precipitates in (a), and (e) FFT pattern of (d).

from a part of the precipitate, which could be ascribed to crystalline apatite with a [$02\bar{1}$] orientation through analysis of the fast Fourier transform (FFT) image (Figure 7e). These results indicate that the apatite crystals nucleated on the dentin surface within 5 min of the LAB process. Taking the EDX results (Figures 1b and 6) into consideration, the fluoride ions were incorporated in the nucleated apatite crystals during the process, *i.e.*, the LAB process induced FAp precipitation on the dentin surface within 5 min. Although a weak *c*-axis orientation was noticed in the underlying dentinal apatite (Figure 7c), it was not apparent in the surface FAp crystals (Figure 7b).

3.2.3 Final stage of the LAB process (30 min)

After the LAB process for 30 min, the FAp nanocrystals grew into a micron-thick layer on the dentin surface. The F, Ca, and P distributions in Figure 8a and the upper STEM-EDX spectrum in

Figure 8c indicated the presence of a dense surface layer consisting of F-incorporated CaP. The surface microlayer had a higher F/P atomic ratio (0.24 ± 0.01) than the underlying dentin (0.08 ± 0.01). In the surface microlayer, F (purple) was distributed homogeneously throughout the CaP matrix (red and green). The surface microlayer was 2−2.5 μm in thickness and integrated seamlessly with the underlying dentin without any interstices or interstitial layers, according to the results of STEM-EDX (Figure 8a) and TEM (lower row images in Figure 5).

The surface microlayer formed on the LAB-processed (30 min) substrate was a FAp layer with *c*-axis orientation along the substrate surface normal. The cross-sectional TEM images in Figures 5 (lower row) and 9a revealed well-developed pillar-like crystals in the surface microlayer, which were densely assembled and oriented vertically to the substrate surface. The top surface of

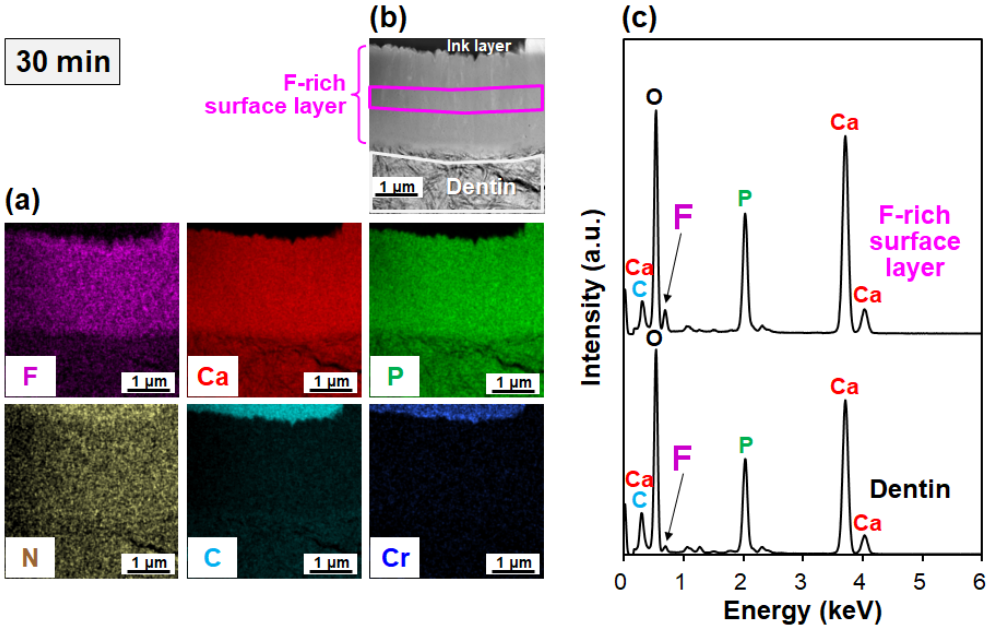

Figure 8. (a) Cross-sectional STEM-EDX elemental maps, (b) corresponding HAADF image, and (c) STEM-EDX spectra of the dentin substrate surface after the LAB process for 30 min. The EDX spectra in (c) were obtained respectively from the F-rich surface layer (purple-boxed region) and dentin (gray-boxed region) in (b).

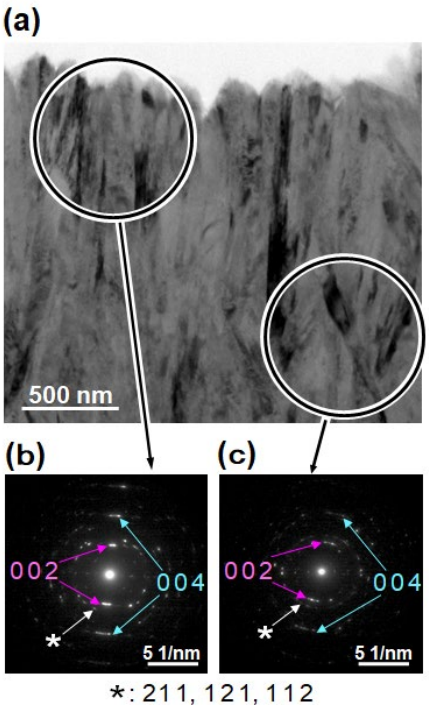

Figure 9. (a) Cross-sectional TEM image of the surface layer formed on the dentin substrate after the LAB process for 30 min and (b,c) SAED patterns obtained from the circled areas in (a).

the layer had submicron roughness due to the vertically assembled pillars with diameters of a few submicrometers. This cross-sectional surface structure agreed well with the top-view SEM image that showed densely assembled submicron particles (see the lower right image in Figure 1a). The pillar-like crystals in the surface microlayer showed the SAED patterns ascribed to apatite, whose *c*-axis was oriented along the direction normal to the substrate surface, based on the 002 and 004 reflections (Figures 9b and 9c). Considering these results together with the EDX results (Figures 1b and 8), the pillar-like crystals in the surface microlayer were confirmed to be FAp crystals, *i.e.*, the dentin substrate was coated with the micron-thick FAp layer after the LAB process for 30 min.

3.3. Area-specific FAp coating capability

The LAB process induced area-specific FAp coating on the dentin substrate. As depicted in the upper left diagram in Figure 10a, we applied the LAB process (30 min) to a partial region (5-mm circular region) of an L-sized substrate surface using a metallic mask. SEM observation of the LAB-processed substrate revealed a smooth boundary between the laser-irradiated (left) and non-irradiated (right) regions (upper image in Figure 10a). As suggested by the magnified SEM images (lower panels in Figure 10a) and EDX spectra (Figure 10b) of each region, the FAp layer was formed only on the laser-irradiated region while the non-irradiated region was left uncoated (see Figure 1 for comparison). This result indicates that the dentin substrate itself has no apatite-forming ability in the FCP solution within the tested immersion period (30 min), which corresponds to our previous result [36]. Therefore, laser irradiation is essential for FAp coating of the dentin surface, as reported for several other substrates [28,30,33,34].

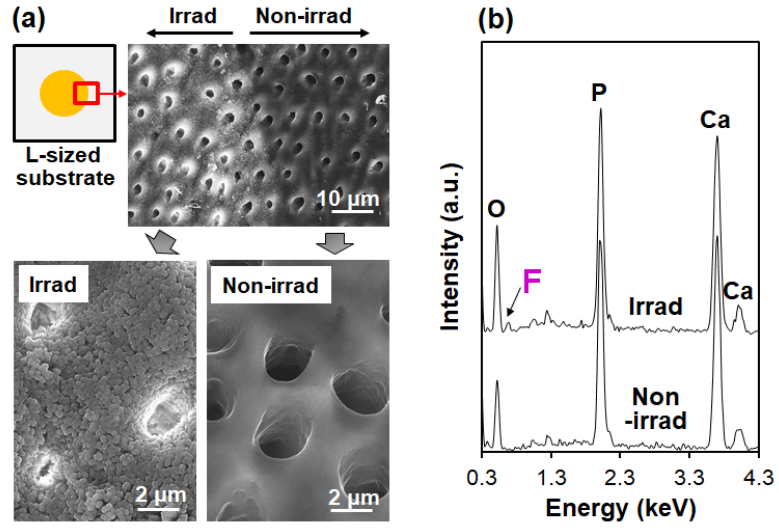

Figure 10. (a) SEM images with lower (upper) and higher (lower) magnification and (b) SEM-EDX spectra of the laser-irradiated and non-irradiated regions on the surface of the L-sized dentin substrate after the LAB process for 30 min.

3.4. Antibacterial assay

The FAp-coated dentin substrate exhibited antibacterial activity against *S. mutans*. The antibacterial activity of the FAp layer was assayed using the LAB-processed (30 min) dentin substrate and the unprocessed substrate as a control. The anaerobic culture of *S. mutans* in the presence of the FAp-coated substrate resulted in a significantly lower CFU value (corresponding to the number of viable bacteria) compared to the control. This result confirmed that the FAp layer coated on the dentin substrate retarded the proliferation of *S. mutans* during culture. Fluoride ions released from the FAp layer are considered to be responsible for the antibacterial activity of the FAp layer [11,34].

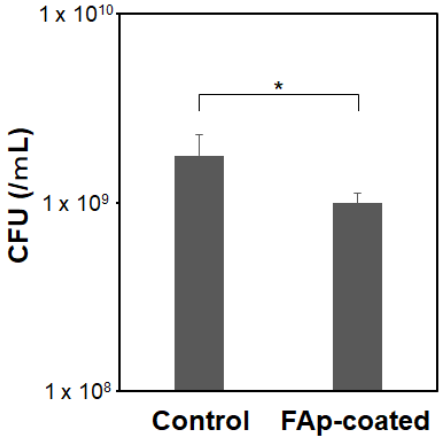

Figure 11. CFU of *S. mutans* after anaerobic culture in the presence of the unprocessed dentin substrate (control) and the FAp-coated dentin substrate that was prepared by the LAB process for 30 min (n=4, average + SD, * $p < 0.05$).

3.5. Putative mechanism

Human dentin substrates were successfully coated with a FAp layer by the present LAB process using the FCP solution. According to the results, the FAp layer was formed heterogeneously on the laser-irradiated solid−liquid interface *via* pseudo-biomineralization in the

presence of fluoride ions. Surface and cross-sectional analyses revealed the time-course for the pseudo-mineralization as follows: The unprocessed (as-prepared) dentin substrate had a submicron-thick N-rich organic layer on its surface (Figure 3), as reported previously [23] through demineralization in the prior cleaning with EDTA. EDTA is a Ca-chelating agent used clinically as a smear removal agent [39]. In the initial stage of the LAB process, this organic layer was rapidly thinned (from *ca.* 300 nm to *ca.* 50 nm in 1 min) and disappeared completely within 5 min (Figures 4 and 6). This is considered to be caused by laser-induced photothermal degradation and ablation of the organic layer [40]. At the same time, fluoride ions in the FCP were incorporated into the dentin surface within 1 min (Figure 4). From the overlap of the F-rich region with the Ca- and P-rich dentinal region (Figure 4a), fluoride ions penetrated though the partially degraded organic layer and were incorporated within the dentinal surface. This fluoride incorporation is most likely due to ionic substitution for hydroxyl ions in the dentinal apatite crystals [9,10]. Although the surface precipitation of CaP crystals was not evident after processing for 1 min, it became apparent after processing for 5 min; nanosized FAp crystals appeared on the LAB-processed (5 min) dentin surface (Figures 5−7). The newly precipitated FAp nanocrystals were different in both composition and size from the underlying dentinal apatite nanocrystals, *i.e.*, the FAp nanocrystals in the surface layer had a higher fluoride content (Figure 6b) and were thicker than the needle-like dentinal apatite nanocrystals (Figure 7a). We consider that FAp nucleated heterogeneously on the dentinal apatite nanocrystals and/or partially degraded organic layer abundant in reactive functional groups. At this stage, the FAp nanocrystals showed no apparent *c*-axis orientation. Precursor phase OCP was not detected under the analytical conditions, probably due to the accelerating effect of fluoride ions on phase transformation into apatite [41,42]. Increasing the processing time to 30 min, the FAp nanocrystals developed into thicker and longer pillar-like FAp

crystals (Figure 5) by the incorporation of Ca and P (ions and/or CaP nanoclusters [43,44]) from the FCP solution (Figure 2a). In this crystal growth stage (5−30 min), the FAp nanocrystals grew, densely packed, and their *c*-axes were aligned vertically to the substrate surface (Figure 9). This phenomenon is known as the geometric selection of crystals [45,46] and has also been observed for the fluoride-free apatite layer formed on a LAB-processed dentin substrate [36]. The final FAp layer was a dense micron-thick FAp layer (Figures 5 and 8).

Laser irradiation played a critical role in the pseudo-biomineralization described here. First, the laser irradiation eliminated the preexisting N-rich organic layer on the dentin substrate, thereby providing active nucleation sites for FAp in the initial stage. This effect accounts for the area-specific coating capability of the LAB process (Figure 10). In addition, the laser irradiation had the effect of accelerating CaP nucleation and crystal growth by heating the surface and the FCP solution. The degree of supersaturation increases in the heated FCP solution because the solubility of apatite decreases above 25 °C [47,48]. The temperature increase in the CP solution during the LAB process was experimentally confirmed using various substrates [28−33]. In the case of the dentin substrate, the CP solution was heated from 25 to 33 °C in the LAB process for 30 min [36]. Besides the laser irradiation effects, fluoride ions added to the FCP solution also led to accelerated CaP nucleation and crystal growth. This is because fluoride ions accelerate the hydrolysis of apatite precursor(s) and increase the driving force for apatite growth by forming thermodynamically more stable and less soluble FAp [42]. In fact, the FAp layer formed in the fluoride-containing FCP solution was thicker (2−2.5 μm, see Figures 5 and 8a) than the apatite layer (less than 1 μm [36]) formed in the fluoride-free CP solution, even though the other LAB processing conditions were identical. Pseudo-biomineralization thus proceeded rapidly on the dentin surface, due to the effects

of laser irradiation and fluoride ions, which led to the formation of a micron-thick FAp layer within only 30 min.

3.6. Expected functionality of the FAp layer

Recently, multifunctional strategies based on the combined use of multiple ingredients have been proposed to develop antibacterial dental materials with the antibacterial property along with other beneficial properties [45]. The FAp layer obtained by the present LAB process would possess multifunctionality owing to the biocompatible apatite matrix and antibacterial fluoride ions as described below.

The FAp layer should exhibit good biocompatibility with periodontal tissues due to the apatite matrix, because of its similarity to the healthy natural tooth and its intrinsic biological characteristics [5−8]. Previously reported apatite-coated polymer substrates prepared using the CP solution showed good biocompatibility with living soft tissue; epidermal downgrowth was prevented compared to an uncoated substrate when implanted percutaneously in a rat scalp [50,51]. In an another report, an apatite-coated titanium implant showed regeneration of periodontal ligament-like tissue around the implant when an occlusal load was applied [52].

The FAp layer should also exhibit antibacterial activity *via* fluoride ion release from the layer. The antibacterial activity of the FAp layer coated on the dentin substrate was confirmed using *S. mutans* (Figure 11). A FAp layer prepared under similar conditions released fluoride ions in a physiological solution at a level (*ca.* 0.2 mg/L at 78 h [34]) higher than the salivary fluoride concentration (0.01−0.1 mg/L [53]); however, this concentration level was still 2 orders of magnitudes lower than the minimum inhibitory concentration for proliferation of oral mucosal

fibroblasts [54]. It should be noted that fluoride ions have a broad antibacterial activity spectrum and are effective for a variety of oral bacteria including periodontopathic bacteria [11].

3.7. Advantages of the present process and future perspective

There are many reports on techniques for the production of an artificially mineralized tooth surface [13-25]. However, each of them has its own strengths and weaknesses, and there is thus a demand for a more practical technique. The LAB process proposed here is a physicochemical process that enables facile (≤30 min) FAp coating on dentin under normal pressure and temperature. The LAB process allows the area-specific coating (Figure 10), which implies that only a targeted region (in millimeter order) of a tooth surface could be treated and coated with FAp. The LAB process requires neither toxic reagents nor specific additives such as proteins, peptides, and dendrimers. The fluoride concentration (1 mM) of the FCP solution is sufficiently low not to raise safety concerns, because it is lower than fluoride concentrations of commercially-available mouth washes [12]. In addition, the overall F dose in the FCP solution (0.09 mg in 5 mL) is 2 orders of magnitudes lower than the tolerable upper intake level (10 mg per day) for humans older than 8 years [55].

If the LAB process for FAp coating is applied to a tooth root surface after surgical periodontal treatment, then the tooth surface would gain good biocompatibility from the apatite matrix along with antibacterial activity from the incorporated fluoride ions. The LAB-processed tooth surface may potentially possess additional functionality because not only fluoride ions but also certain other bioactive ingredients such as fibronectin and zinc can be immobilized on the surface by the addition of these ingredients to the CP solution [32]. This is an advantageous feature of biomimetic processes that use supersaturated CaP solutions as a reaction medium. The FAp-coated tooth

surface would be sealed with the gingival tissue after surgery. Under the resulting static environment at the root–gingiva interface (region unaffected by daily mastication and brushing), the FAp layer would persist for a certain period. This is because the body fluid is highly supersaturated with respect to FAp. According to our previous study [34], a FAp layer prepared under similar conditions exhibited higher chemical stability (acid-resistance) than a non-resorbable sintered hydroxyapatite ceramic. The LAB process produced an antibacterial tooth surface where the top FAp layer was integrated seamlessly with the underlying dentin without any apparent gaps (Figures 5 and 8). Such a functionalized tooth surface would help the reconstruction of periodontal attachment, prevent bacterial proliferation, and thus reduce the risk of recurrence. *In vitro* and *in vivo* studies are required to verify this hypothesis. Further process refinement and evaluation of the coating layer (*e.g.*, adhesion strength, mechanical properties, and chemical durability) are also necessary.

4. Conclusion

Human dentin substrates were successfully coated with a micron-thick FAp layer using the LAB process for 30 min with FCP solution. The FAp layer was formed heterogeneously at the laser-irradiated solid−liquid interface *via* pseudo-biomineralization in the presence of fluoride ions. In this process, laser irradiation eliminated the pre-existing organic layer and allowed fluoride incorporation into the dentin surface within 1 min. FAp nanocrystals precipitated at the dentin surface within 5 min and grew into pillar-like FAp nanocrystals with a weak c-axis orientation along the surface normal within 30 min. The resulting FAp layer was integrated seamlessly with the underlying dentin without gaps, and also exhibited antibacterial activity against *S. mutans*. The

proposed LAB process is expected to be a useful new tool for tooth surface functionalization *via* facile and area-specific pseudo-biomineralization.

Acknowledgments

This work was supported by JSPS KAKENHI (JP17H02093, JP19K22991, JP20H04541). The authors thank Mr. N. Saito and Dr. N. Yoshizawa from AIST for conducting TEM analyses, and Dr. M. Zhang and Ms. K. Kuroiwa from AIST for ICP-OES measurements.

References

[1] B.L. Pihlstrom, B.S. Michalowicz, N.W. Johnson, Periodontal diseases, Lancet 366 (2005) 1809–1820.

[2] S.S. Steiner, M. Crigger, J. Egelberg, Connective tissue regeneration to periodontally diseased teeth, J. Periodont. Res. 16 (1981) 109–116.

[3] J. Caton, S. Nyman, Histometric evaluation of periodontal surgery l. The modified Widman flap procedure, J. Clin. Periodontol. 7 (1980) 224–231.

[4] T. Fujita, S. Yamamoto, M. Ota, Y. Shibukawa, S. Yamada, Coverage of gingival recession defects using guided tissue regeneration with and without adjunctive enamel matrix derivative in a dog model, Int. J. Periodont. Restorative Dent. 31 (2011) 247–253.

[5] R.A. Surmenev, M.A. Surmeneva, A.A. Ivanova, Significance of calcium phosphate coatings for the enhancement of new bone osteogenesis – A review, Acta Biomaterialia 10 (2014) 557–579.

[6] S.V. Dorozhkin, Calcium orthophosphate deposits: Preparation, properties and biomedical applications, Mater. Sci. Eng. C 55 (2015) 272–326.

[7] W. Habraken, P. Habibovic, M. Epple, M. Bohner, Calcium phosphates in biomedical applications: materials for the future?, Mater. Today 19 (2016) 69–87.

[8] H.L. Oliveira, W.L.O. Da Rosa, C.E. Cuevas-Suárez, N.L.V. Carreño, A.F. da Silva, T.N. Guim, O.A. Dellagostin, E. Piva, Histological evaluation of bone repair with hydroxyapatite: A systematic review, Calcif. Tissue Int. 101 (2017) 341–354.

[9] L.A. Aponte-Merced, F.F. Feagin, Effect of fluoride on ion exchange, remineralization and acid resistance of surface enamel, J. Oral Pathol. 8 (1979) 333–339.

[10] I. Manjubala, M. Sivakumar, S.N. Nikkath, Synthesis and characterization of hydroxy/fluoroapatite solid solution, J. Mater. Sci. 36 (2001) 5481–5486.

[11] R.E. Marquis, Antimicrobial actions of fluoride for oral bacteria, Can. J. Microbiol. 41 (1995) 955–964.

[12] R. Ullah, M.S. Zafar, Oral and dental delivery of fluoride: a review, Fluoride 48 (2015) 195–204.

[13] E. Yamamoto, N. Kato, S. Hontsu, Adhesive evaluation by brushing tests for hydroxyapatite films fabricated on dentins using a water mist assisted Er:YAG laser deposition method, Key Eng. Mater. 758 (2017) 97–104.

[14] K. Izumita, R. Akatsuka, A. Tomie, C. Kuji, T. Kuriyagawa, K. Sasaki, Development of powder jet deposition technique and new treatment for discolored teeth, in: K. Sasaki, O. Suzuki, N. Takahashi (Eds.), Interface Oral Health Science 2016, Springer, Singapore, 2017, pp. 257–267.

[15] S. Hontsu, K. Yoshikawa, 6 - Ultra-thin hydroxyapatite sheets for dental applications, in M. Mucalo (Ed.), Hydroxyapatite (Hap) for Biomedical Applications, Woodhead Publishing Series in Biomaterials, Elsevier, Cambridge, 2015, pp. 129–142.

[16] K. Yamagishi, K. Onuma, T. Suzuki, F. Okada, J. Tagami, M. Otsuki, P. Senawangse, A synthetic enamel for rapid tooth repair, Nature 433 (2005) 819.

[17] Y. Fan, J.R. Nelson, J.R. Alvarez, J. Hagan, A. Berrier, Amelogenin-assisted ex vivo remineralization of human enamel: Effects of supersaturation degree and fluoride concentration, Acta Biomaterialia, 7 (2011) 2293–2302.

[18] L. Li, C. Mao, J. Wang, X. Xu, H. Pan, Y. Deng, X. Gu, R. Tang, Bio-inspired enamel repair via Glu-directed assembly of apatite nanoparticles: an approach to biomaterials with optimal characteristics, Adv. Mater. 23 (2011) 4695–4701.

[19] H.Y. Chung, C.C. Li, C.C. Hsu, Characterization of the effects of 3DSS peptide on remineralized enamel in artificial saliva, J. Mech. Behab. Biomed. 6 (2012) 74–79.

[20] D. Wu, J. Yang, J. Li, L. Chen, B. Tang, X. Chen, W. Wu, J. Li, Hydroxyapatite-anchored dendrimer for in situ remineralization of human tooth enamel, Biomater. 34 (2013) 5036–5047.

[21] L. Niu, W. Zhang, D.H. Pashley, L. Breschi, J. Mao, J. Chen, F.R. Tay, Biomimetic remineralization of dentin, Dent. Mater. 30 (2014) 77–96.

[22] S.Y. Kwak, A. Litman, H.C. Margolis, Y. Yamakoshi, J.P. Simmer, Biomimetic enamel regeneration mediated by leucine-rich amelogenin peptide, J. Dent. Res. 96 (2017) 524–530.

[23] A. Shao, B. Jin, Z. Mu, H. Lu, Y. Zhao, Z. Wu, L. Yan, Z. Zhang, Y. Zhou, H. Pan, Z. Liu, R. Tang, Repair of tooth enamel by a biomimetic mineralization frontier ensuring epitaxial growth, Sci. Adv. 5 (2019) eaaw9569.

[24] M. Sun, N. Wu, H. Chen, Laser-assisted rapid mineralization of human tooth enamel, Sci. Rep. 7 (2017) 9611.

[25] E. Soltanimehr, E. Bahrampour, Z. Yousefvand, Efficacy of diode and CO_2 lasers along with calcium and fluoride-containing compounds for the remineralization of primary teeth, BMC Oral Health, 19 (2019) 121.

[26] M. Nakamura, A. Oyane, Physicochemical fabrication of calcium phosphate-based thin layers and nanospheres using laser processing in solutions, J. Mater. Chem. B 4 (2016) 6289–6301.

[27] M. Uchida, A. Oyane, H.M. Kim, T. Kokubo, A. Ito, Biomimetic coating of laminin–apatite composite on titanium metal with excellent cell adhesive property, Adv. Mater. 16 (2004) 1071–1074.

[28] A. Oyane, I. Sakamaki, Y. Shimizu, K. Kawaguchi, N. Koshizaki, Liquid-phase laser process for simple and area-specific calcium phosphate coating, J. Biomed. Mater. Res. A 100A (2012) 2573–2580.

[29] A. Oyane, A. I. Sakamaki, Y. Shimizu, K. Kawaguchi, Y. Sogo, A. Ito, N. Koshizaki, Laser-assisted biomimetic process for calcium phosphate coating on a hydroxyapatite ceramic, Key Eng. Mater. 529–530 (2013) 217–222.

[30] A. Oyane, I. Sakamaki, A. Pyatenko, M. Nakamura, Y. Ishilawa, K. Kawaguchi, N. Koshizaki, Laser-assisted calcium phosphate deposition on polymer substrates in supersaturated solutions, RSC Adv. 4 (2014) 53645–53648.

[31] M. Mahanti, M. Nakamura, A. Pyatenko, I. Sakamaki, K. Koga, A. Oyane, The mechanism underlying calcium phosphate precipitation on titanium via ultraviolet, visible, and near infrared laser-assisted biomimetic process, J. Phys. D: Appl. Phys. 49 (2016) 304003.

[32] A. Oyane, N. Matsuoka, K. Koga, Y. Shimizu, M. Nakamura, K. Kawaguchi, N. Koshizaki, Y. Sogo, A. Ito, H. Unuma, Laser-assisted biomimetic process for surface functionalization of titanium metal, Coll. Interf. Sci. Comm. 4 (2015) 5–9.

[33] A. Oyane, M. Nakamura, I. Sakamaki, Y. Shimizu, S. Miyata, H. Miyaji, Laser-assisted wet coating of calcium phosphate for surface-functionalization of PEEK, PLoS ONE 13 (2018) e0206524.

[34] A.J. Nathanael, A. Oyane, M. Nakamura, K. Shitomi, H. Miyaji, Rapid and area-specific coating of fluoride-incorporated apatite layers by a laser-assisted biomimetic process for tooth surface functionalization, Acta Biomaterialia 79 (2018) 148–157.

[35] A.J. Nathanael, A. Oyane, M. Nakamura, K. Koga, E. Nishida, S. Tanaka, H. Miyaji, Calcium phosphate coating on dental composite resins by a laser-assisted biomimetic process, Heliyon 4 (2018) e00734.

[36] A. Oyane, N. Saito, I. Sakamaki, K. Koga, M. Nakamura, A.J. Nathanael, N. Yoshizawa, K. Shitomi, K. Mayumic, H. Miyaji, Laser-assisted biomineralization on human dentin for tooth surface functionalization, Mater. Sci. Eng. C 105 (2019) 110061.

[37] D.J. Bradshaw, P.D. Marsh, K. Watson, C. Allison, Role of fusobacterium nucleatum and coaggregation in anaerobe survival in planktonic and biofilm oral microbial communities during aeration, Infect. Immun. 66 (1998) 4729–4732.

[38] J.A. Lemos, S.R. Palmer, L. Zeng, Z.T. Wen, J.K. Kajfasz, I.A. Freires, J. Abranches, L.J. Brady, The Biology of Streptococcus mutans, Microbiol. Spectr. 7 (2019) GPP3-0051-2018.

[39] Z. Mohammadi, S. Shalavi, H. Jafarzadeh, Ethylenediaminetetraacetic acid in endodontics, Eur. J. Dent. 7 (Suppl 1) (2013) S135–S142.

[40] N. Arnold, N. Bityurin, Model for laser-induced thermal degradation and ablation of polymers, Appl. Phys. A 68 (1999) 615–625.

[41] M. Iijima, K. Onuma, Roles of fluoride on octacalcium phosphate and apatite formation on amorphous calcium phosphate substrate, Cryst. Growth Design, 18 (2018) 2279–2288.

[42] T. Aoba, The effect of fluoride on apatite structure and growth, Crit. Rev. Oral Biol. Med. 8 (1997) 136–153.

[43] K. Onuma, A. Ito, Cluster growth model for hydroxyapatite, Chem. Mater. 10 (1998) 3346–3351.

[44] A. Dey, P.H.H. Bomans, F.A. Müller, J. Will, P.M. Frederik, G. de With, N.A.J.M. Sommerdijk, The role of prenucleation clusters in surface-induced calcium phosphate crystallization, Nat. Mater. 9 (2010) 1010–1014.

[45] Y. Jiao, F.R. Tay, L. Niu, J. Chen, Advancing antimicrobial strategies for managing oral biofilm infections, Int. J. Oral Sci. 11 (2019) 28.

[46] C.V. Thompson, Structure evolution during processing of polycrystalline films, Annu. Rev. Mater. Sci. 30 (2000) 159–190.

[47] K. Onuma, M. Iijima, Artificial enamel induced by phase transformation of amorphous nanoparticles, Sci. Rep. 7 (2017) 2711.

[48] H. McDowell, T. Gregory, W. Brown, Solubility of $Ca_5(PO_4)_3OH$ in the system $Ca(OH)_2$–H_3PO_4–H_2O at 5, 15, 25 and 37°C, J. Res. Nat. Bureau Stand. 81 (1972) 273–281.

[49] M.J.J.M. Van Kemenade, P.L. De Bruyn, A kinetic study of precipitation from supersaturated calcium phosphate solutions, J. Col. Interf. Sci. 118 (1987) 564–585.

[50] A. Oyane, K. Hyodo, M. Uchida, Y. Sogo, A. Ito, Preliminary in vivo study of apatite and laminin-apatite composite layers on polymeric percutaneous implants, J. Biomed. Mater. Res. B, 97B (2011) 96-104.

[51] K. Sasaki, A. Oyane, K. Hyodo, A. Ito, Y. Sogo, M. Kamitakahara, K. Ioku, Preparation and biological evaluation of a fibroblast growth factor-2–apatite composite layer on polymeric material, Biomed. Mater. 5 (2010) 065008.

[52] T. Kano, R. Yamamoto, A. Miyashita, K. Komatsu, T. Hayakawa, M. Sato, S. Oida, Regeneration of periodontal ligament for apatite-coated tooth-shaped titanium implants with and without occlusion using rat molar model, J. Hard Tissue Biol. 21 (2012) 189–202.

[53] K.J. Toumba, M.E.J. Curzon, Fluoride concentrations in saliva related to dental caries prevalence in primary teeth, European J. Paediatric Dentistry 2 (2001) 15–19.

[54] J.H. Jeng, C.C. Hsieh, W.H. Lan, M.C. Chang, S.K. Lin, L.J. Hahn, M.Y.P. Kuo, Cytotoxicity of sodium fluoride on human oral mucosal fibroblasts and its mechanisms, Cell Biol. Toxicol. 14 (1998) 383–389.

[55] Standing Committee on the Scientific Evaluation of Dietary Reference Intakes, Food and Nutrition Board, Institute of Medicine, Dietary Reference Intakes for Calcium, Phosphorus, Magnesium, Vitamin D, and Fluoride, National Academies Press, Washington D.C., 1997, pp. 306–313.